Charge-exchange processes in titanium-doped sapphire crystals. II. Charge-transfer transition states, carrier trapping, and detrapping

Wing C. Wong and Donald S. McClure
Department of Chemistry, Princeton University, Princeton, New Jersey 08544

Sergei A. Basun
A. F. Ioffe Physicotechnical Institute, Academy of Sciences of Russia, 194021, St. Petersburg, Russian Federation

Milan R. Kokta
Union Carbide, Chemicals and Plastics Company Inc., 750 South 32 Street, Washougal, Washington 98671

(Received 19 September 1994)

From the time-resolved emissions of the Ti^{4+}:Al_2O_3 charge-transfer transition, two types of Ti^{4+} are found. The temperature-dependent lifetimes of the excited Ti^{4+} are well explained by a three-level system with a lower triplet excited state and a higher singlet excited state. The trapping of charge carriers following the charge exchange between Ti and the host is shown by the thermal release of trapped electrons and holes. These are revealed by thermally stimulated conductivity and thermoluminescence. The possible identities of these traps are discussed.

I. INTRODUCTION

Two types of Ti^{4+} ions in Al_2O_3 (locally and nonlocally charge compensated) are identified optically. The lifetimes of the charge-transfer (CT) emission as a function of temperature are well explained by assuming a triplet excited state that is in thermal equilibrium with the higher singlet excited state. From these multiplets, a correction of 0.1 eV is made to the CT energy threshold found in part I.[1]

In part I and Ref. 2, the photochemical products of Ti-Al_2O_3 charge exchange become observable in the low-energy region of the photoconductivity spectra. The results on thermally stimulated conductivity and thermoluminescence (TL) obtained here show that this is due to trapped electrons generated from Ti^{3+} photoionization (PI). In addition, trapped holes originating from the oxide to Ti^{4+} charge-transfer (CT) transition are also detected in TL.

The TL result from V^{4+},Mg^{2+}:Al_2O_3 indicates that the electron traps are not the intrinsic defects of Al_2O_3. The result on Ti^{4+},Mg^{2+}:Al_2O_3 suggests that the hole traps are the negatively charged compensators for the Ti^{4+} ions.

II. EXPERIMENT

A. Sample preparation and characterization

The growing conditions and optical characterization of the crystals are detailed in part I.[1] It should be mentioned here that the two Ti:Al_2O_3 crystals used have very different relative concentrations of Ti^{3+} and Ti^{4+} (sample *A* contains 2.1×10^{19} cm^{-3} Ti^{3+} and 2.9×10^{18} cm^{-3} Ti^{4+} while sample *B* contains 5.9×10^{18} cm^{-3} Ti^{3+} and 7.3×10^{16} cm^{-3} Ti^{4+}). In addition, a thin slice of Ti,Mg-codoped sapphire (sample *C*) in which titanium exists as Ti^{4+} (5×10^{18} cm^{-3}) was also studied. Using a 3.1-cm-thick codoped sample, it is found that the concentration of Ti^{3+} in sample *C* is $<7\times10^{17}$ cm^{-3}. Also, the intensity of the IR band (assigned to Ti^{3+}-Ti^{4+} pairs) (Ref. 3) peaking at 800 nm is comparable to the *d-d* absorption band in the codoped sample.

B. Time-resolved emission and luminescence excitation

Emission at 300 K was excited with 10-ns 240-nm laser pulses generated from frequency doubling the output of a Lambda Physik FL 3002 dye laser. The time-resolved spectra were taken using an ISA DH-10 double monochromator and a Hamamatsu R928 PMT. The signal was averaged and recorded with a Nicolet 4094C digital oscilloscope. The spectral response of the detection system was measured and corrections were applied. The luminescence excitation spectra were taken at 300 K with a Perkin Elmer Model LS 50 spectrometer.

C. Thermally stimulated conductivity

The sample was kept between two nickel mesh electrodes, which are insulated from the grounded holder with two supersil grade quartz plates. The sample holder was attached to a cold finger. The current was measured with a Cary 401 vibrating reed electrometer with a typical noise level of 10^{-15} A. Initially, the sample was kept at 77 K in the presence of an electric field and irradiated with UV light (230 nm). The charge carriers generated are trapped downfield. After the irradiation was completed, the electric field was turned off and the circuit was grounded through the electrometer. As the temperature was raised, the depolarization current was recorded. Due to the dielectric hysteresis of the insulating materials in the sample holder, there was always some background signal (sharp peaks between 300 and 320 K). Hence, dark runs were taken and subtracted from the signal.

D. Thermally stimulated luminescence

The sample was kept at 77 K and irradiated for a known period of time at different wavelengths (230–470

nm, bandwidth = 8 nm). Then, the temperature was increased at a rate of about 4 K per min. The signal was detected by a thermoelectrically cooled RCA C31034 GaAs photomultiplier (PMT). Photon counts were recorded as a function of temperature. The spectral distribution of the thermoluminescence peak(s) was obtained by inserting different cutoff/bandpass filters in front of the PMT.

For each run, the area under the peak(s) was integrated with respect to time. Then, it was normalized by the total number of incident UV photons during the irradiation. When different filters were used, the ratio of signal with and without the filter was calculated.

III. RESULTS AND DISCUSSION

A. Emission and excitation spectra of Ti^{4+}

Figure 1 shows the time-resolved 470-nm emission at room temperature for sample *A* excited at 240 nm. The emission can be resolved into two components with lifetimes of about 4 μs and 30 μs, respectively. Similarly, sample *B* showed a very weak 3.5 μs and a stronger 35 μs emission. The spectral distribution of the two emitting components are shown in Fig. 2(a).

The two UV excited blue emissions in Ti:Al_2O_3 were reported before.[4,5] The fast component was attributed to Ti^{3+} while the slow component was attributed to Ti^{4+}. We have investigated the 240-nm excited emission from the Ti,Mg-codoped sapphire (sample *C*), whose emission also showed two components with lifetimes similar to those of the singly doped samples (6 μs and 38 μs). Thus, contrary to the previous interpretations in Refs. 4 and 5, the fast component appears to be related to Ti^{4+}. Actually, from the absorption spectrum in Ref. 5, it can be estimated that the concentration of Ti^{3+} is 0.008 mol % (agrees well with the authors' reported 0.01 wt. %) but at the same time, the sample contains a substantial amount of Ti^{4+} (0.02 mol %) that can be the sources of the blue emissions. In fact, from the two emission bands (410 and 480 nm) of an oxygen annealed 0.03 at. % Ti:Al_2O_3, it was suggested that the two bands are due to the isolated

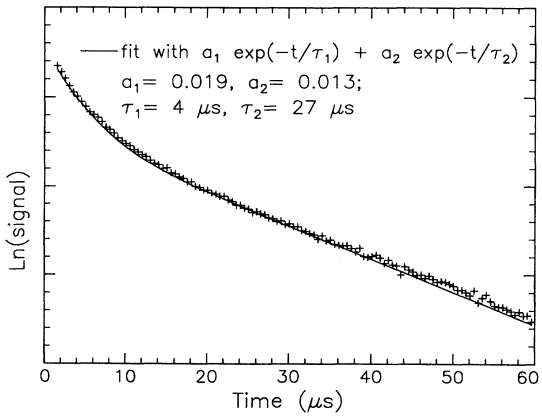

FIG. 1. Time-resolved 470-nm emission of sample *A* excited with 240-nm laser pulse at 300 K.

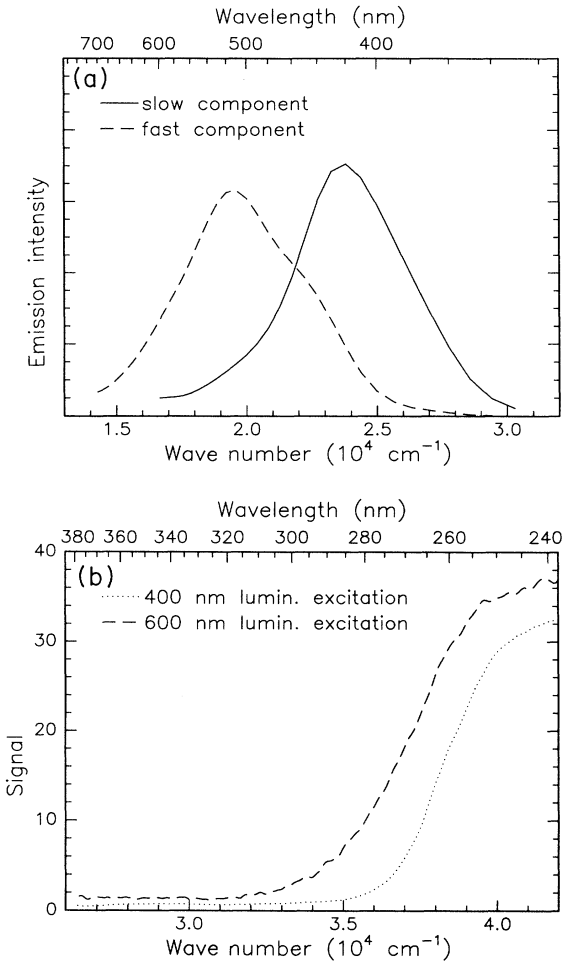

FIG. 2. (a) The two UV-excited emitting components of the two Ti:Al_2O_3 samples. The 420- and 460-nm bands shown here are from sample *A* and sample *C*, respectively. (b) Luminescence excitation spectra (ordinate axis in arbitrary units) of the Ti^{4+},Mg^{2+}:Al_2O_3 sample.

Ti^{4+} and Ti^{4+} associated with the Al^{3+} vacancy.[6] The discussion below provides further support for this argument.

Quantitatively, at room temperature, the integrated emission intensity ratios of the fast to the slow component are 1/150, 1/9, and 1.2/1 for sample *B*, sample *A*, and sample *C*. As the amount of Ti^{4+} increases (from sample *B* to sample *A* to sample *C*), the average distance between the Ti^{4+} and the charge compensator decreases. As a result, the percentage of locally compensated to nonlocally compensated Ti^{4+} should increase. Thus, based on the trend of the integrated intensity ratios, the slow component and fast components are assigned to the nonlocally compensated Ti^{4+} and locally compensated Ti^{4+}, respectively. That the lifetimes of the slow component in all three samples are almost identical is explained because these centers are all nonlocally compensated Ti^{4+}. The lifetime of the fast component is slightly different since in the doubly doped samples, Mg'_{Al} is the

charge compensator while in the singly doped samples, intrinsic defects [most likely the negatively charged aluminum vacancies, V_{Al}''' (Ref. 7)] are the charge compensators. That the fast component due to the compensated Ti^{4+} emits at the lower-energy range [Fig. 2(a)] is consistent with its structure: the presence of the negatively charged compensator reduces the charge-transfer threshold. The oxide ions near the Mg^{2+} have their electron orbital energies raised, i.e., there is smaller binding in the vicinity of the less positively charged Mg^{2+} compared to an Al^{3+}. It is assumed that Mg^{2+} is at the nearest-neighbor site of the Ti^{4+}. From the 400- and 600-nm emission excitation spectra for the Ti,Mg:Al_2O_3 sample [Fig. 2(b)], the energy shift is found to be about 2000 cm^{-1}.

B. Triplet and singlet charge-transfer states

Based on the emission lifetimes of 30 and 4 μs, the oscillator strengths, $f=1.5/v^2\tau$, are expected to be 5×10^{-5} and 3×10^{-4}. However, the reported absorption cross section (28×10^{-18} cm^2) for the Ti^{4+} absorption band[8] leads to an estimated oscillator strength of 0.1. This discrepancy can be explained by the absorption being a spin-allowed transition from the

$$^1A_{1g}\{[Ti^{4+}(t_{2g}^0e_g^0),{}^1A_{1g}][O_6^{12-},{}^1A_{1g}]\}$$

ground state to one of the lowest $^1T_{1u}$ states, e.g.,

$$^1T_{1u}\{[Ti^{3+}(t_{2g}^1e_g^0),{}^2T_{2g}][O_6^{11-},{}^2T_{1u}]\}\ .$$

The lowest emitting states are the corresponding triplet states, which explains the relatively slow decay rate at lower temperature. The decreasing lifetime as temperature increases for the slow component (for nonlocally compensated Ti^{4+}) is a result of increasing intersystem crossing rate between the singlet and triplet states. Because of the large bandwidth, singlet and triplet emissions are not distinguishable. Figure 3(a) shows the radiative decay rate of the 420-nm band as a function of temperature (from Ref. 4). The inset shows the schematic energy levels for the nonlocally compensated Ti^{4+}. N_0, N_1, and N_3 are the population in the singlet ground state, the singlet excited state, and the triplet excited state, respectively. k_{10} and k_{30} are the radiative decay rate constants for the singlet and triplet excited states. The rate of nonradiative intersystem crossing, k_{13} and k_{31} are related by $k_{31}=(k_{13}/3)e^{-E_a/kT}$. Then we have

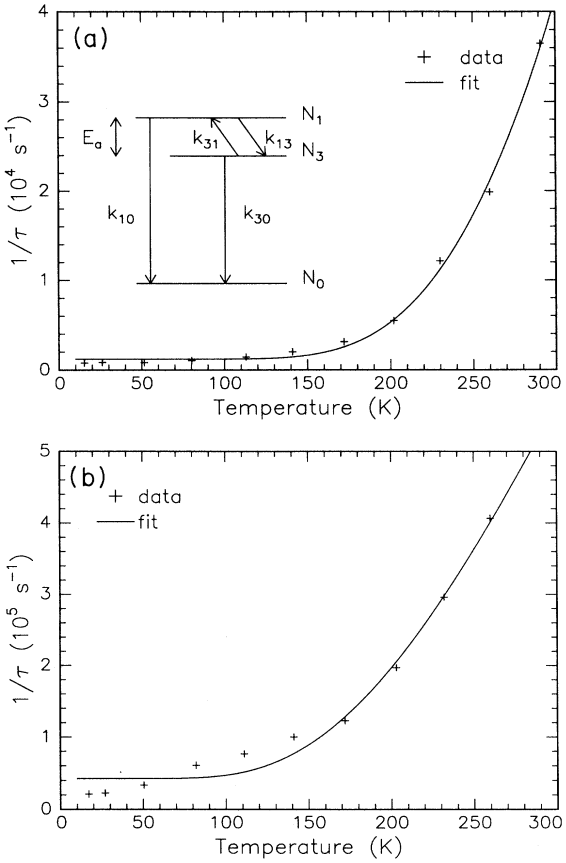

FIG. 3. Temperature dependence of the reciprocal lifetime for the CT band. The fitting assumes the lower triplet state is in thermal equilibrium with the higher singlet state. (a) 420-nm band of the nonlocally compensated Ti^{4+}. (b) 460-nm band of the locally compensated Ti^{4+}.

$$\frac{dN_1(t)}{dt}=-k_{10}N_1(t)-k_{13}N_1(t)+k_{31}N_3(t)\ , \tag{1}$$

$$\frac{dN_3(t)}{dt}=k_{13}N_1(t)-k_{31}N_3(t)-k_{30}N_3(t)\ . \tag{2}$$

Solving Eqs. (1) and (2), the time evolution of the emission, $I(t)$, is

$$k_{10}N_1(t)+k_{30}N_3(t)=C_1e^{-[(R-S)/2]t}+C_2e^{-[(R+S)/2]t}\ , \tag{3}$$

where $R=k_{10}+k_{13}+k_{30}+k_{31}$ and

$$S=\sqrt{(k_{10}+k_{13})^2+(k_{30}+k_{31})^2+2(k_{13}k_{31}-k_{10}k_{30}-k_{13}k_{30}-k_{10}k_{31})}$$

and C_1, C_2, are expressions depending on the initial populations $N_1(0)$, $N_3(0)$,

$$C_1=\frac{N_1(0)[k_{10}S+k_{10}k_{30}+k_{10}k_{31}+2k_{13}k_{30}-k_{10}^2-k_{10}k_{13}]+N_3(0)[k_{30}S+k_{10}k_{30}+k_{13}k_{30}+2k_{10}k_{31}-k_{30}^2-k_{30}k_{31}]}{2S},$$

$$C_2=\frac{N_1(0)[k_{10}S-k_{10}k_{30}-k_{10}k_{31}-2k_{13}k_{30}+k_{10}^2+k_{10}k_{13}]+N_3(0)[k_{30}S-k_{10}k_{30}-k_{13}k_{30}-2k_{10}k_{31}+k_{30}^2+k_{30}k_{31}]}{2S}.$$

The second term in Eq. (3) is a very fast decaying component that is mostly due to the singlet radiative rate, while $(R-S)/2$ in the first term corresponds to the reported emitting rate of the 420-nm band. The solid line in Fig. 3(a) is the result of fitting $1/\tau$ with $(R-S)/2$. The nonlinear least-squares fit gives $k_{10}=7\times10^{7}$ s^{-1}, $k_{30}=1.2\times10^{3}$ s^{-1}, $k_{13}=1.4\times10^{7}$ s^{-1}, and $E_a=950$ cm^{-1}. The ratio $k_{30}/k_{10}=6\times10^{-4}$ can be understood in terms of the singlet-triplet mixing. An order of magnitude estimate is given by

$$\left[\frac{\zeta_{3d}(\mathrm{Ti})}{E_S-E_T}\right]^2=\left[\frac{50}{1000}\right]^2=25\times10^{-4},$$

where E_S-E_T is the singlet-triplet separation and $\zeta_{3d}(\mathrm{Ti})$ is the spin-orbit parameter calculated from the multiplet splitting of the $^2T_2$ ground state of Ti^{3+}. A more accurate estimate would have to include the effects of the large Huang-Rhys factor of these transitions and more details of the charge transfer wave functions.

For the compensated Ti^{4+} (460-nm band), the fitting gives [Fig. 3(b)] $k_{10}=8\times10^{7}$ s^{-1}, $k_{30}=4.2\times10^{4}$ s^{-1}, $k_{13}(0)=2.2\times10^{7}$ s^{-1}, and $E_a=500$ cm^{-1}. The larger value for k_{30} and the smaller E_a are probably due to the presence of the charge compensator.

C. Charge-transfer energy threshold

In part I,[1] we estimated the zero-phonon line of the charge-transfer process from the luminescence excitation of Ti^{4+} and the corresponding fluorescence. There is a correction, however, which arises from the fact that the observed charge-transfer band does not correspond to the appearance of Ti^{3+} infinitely separated from the hole in the O^{2-} lattice.[9] The hole is localized on the six near-neighbor O^{2-} ions. The $3d$ electron on Ti interacts with this hole to form a multiplet. Sec. III B above shows that the triplet excited state is about 1000 cm^{-1} below the singlet excited state. Therefore, the weighted average of the singlet and triplet levels gives a correction of about $-\frac{3}{4}\times1000$ cm$^{-1}=-0.1$ eV to the estimated zero-phonon line position (see Part I, Table II).[1]

D. Thermally stimulated conductivity

The thermally stimulated conductivity for sample *B* is shown in Fig. 4. It is assumed that retrapping does not occur and that the lifetimes of the carriers are constant with a single trap depth of E.[10] The detrapping can be described by the first-order kinetics,

$$\tau(T)=\tau_0 e^{E/kT}, \tag{4}$$

where $\tau(T)$ is the reciprocal of the trapping rate at temperature T. It follows that the current signal has a functional form which is similar to that used in the ionic thermal current (ITC) analysis.[11,12]

$$\ln\tau(T)=\ln\tau_0+\frac{E}{kT} \tag{5}$$

and

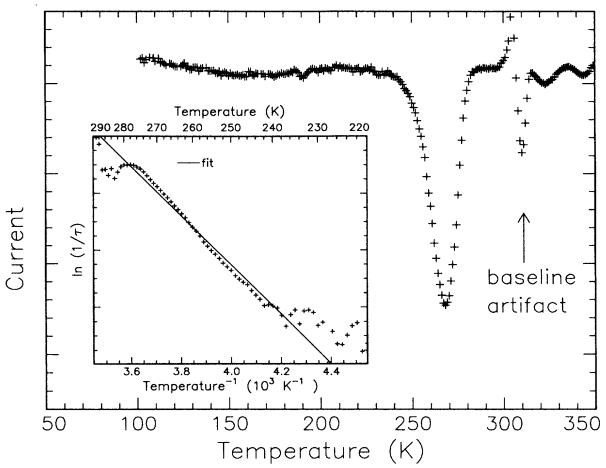

FIG. 4. Thermally stimulated conductivity of sample *B* following 230-nm irradiation.

$$\ln\tau(T)=\ln\left\{\frac{\int_{t(T)}^{t(\infty)}I(t)dt}{I(T)}\right\}. \tag{6}$$

Assuming a frequency factor of 10^{13} s^{-1} (≈300 cm^{-1}), the fitting (Fig. 4 inset) gave a value of 0.74 eV for the trap depth. The thermoluminescence results presented below confirmed that the thermally stimulated conductivity is due to the electron detrapping rather than ionic relaxation since the latter would not give rise to any emission.

E. Thermoluminescence

Results for the two samples are shown in Fig. 5. The peaks at 168 K gave blue light and the peaks at 256 K gave red. Through the use of different band pass and cutoff filters, the emissions were found to be similar to the Ti^{3+} $d-d$ emission and the Ti^{4+} CT emission measured before. As a result, the 168-K blue peak is due to the thermal release of trapped holes while the 256-K red peak is related to trapped electrons. The integrated intensity of the blue peak was about 100 times stronger in sample *A* than in sample *B*. The 256-K red thermoluminescence peak was about 500 times stronger in sample *B*. This result can be understood since with less Ti^{4+}, more photons are absorbed by Ti^{3+} in sample *B*. In addition, the smaller amount of Ti^{4+} increases the probability of the electron being stored by shallow traps.

The red 256-K peak vanished when the excitation wavelength was above 270 nm for sample *A*. This is in accord with the photoionization threshold found from photoconductivity measurements.[1] However, the signal for sample *B* extended down to 450 nm. This suggests the presence of other deeper traps (e.g., *F* centers) which were thermally stable but ionizable by light. For the blue peak, the intensity vanished at about 330 nm, which is close to the charge-transfer threshold for Ti^{4+} in Al_2O_3.[1]

Again, assuming τ_0 to be 10^{13} s^{-1} in Eq. (6), the fittings yield trap depths of 0.44 and 0.71 eV for the peaks at 168

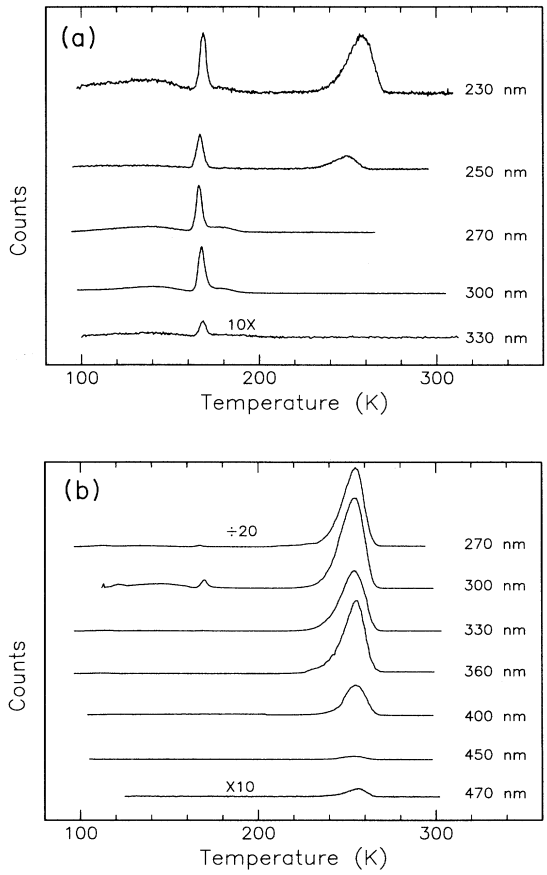

FIG. 5. Thermoluminescence spectra of (a) sample *A*, (b) sample *B*.

and 256 K, respectively. Note that both the peaking temperature and trap depth of the red peak are close to the values obtained from the thermally stimulated conductivity in Sec. III D above. The 168-K blue emission peak does not have an analogue in the thermally stimulated conductivity. Its absence is consistent with the low mobility (larger effective mass) of holes in Al_2O_3.[13] Also, the neighboring charge compensator for the Ti^{4+} could be a deep trap for the holes (see below), rendering the average range of the hole to be small.

To further prove that the 256-K red peak is associated with the trapped electrons following Ti^{3+} photoionization, the selectivity of two-step photoionization was utilized. We observed that after irradiating sample *A* at 77 K using coincident laser pulses at 532 and 355 nm, a small but reproducible thermoluminescence peak at 250 K was formed. As a control experiment, the sample was irradiated with 355-nm pulses and then followed by 532-nm pulses for the same period of time. No signal was observable for the control. As the two-step photoionization causes only Ti^{3+} PI but not Ti^{4+} CT, this shows that the 250-K TL peak is correlated with electrons.

In thermochemically colored undoped sapphire (with *F* and F^+ centers), a 0.73-eV deep electron trap was reported which is the origin of a 260-K thermoluminescence.[14] This is not very different from the 256 K thermoluminescence peak found here in the Ti:sapphire samples. It is possible that the free carrier trapping in the undoped and doped sapphires are both due to the intrinsic defect(s) of Al_2O_3 (e.g., oxide vacancy and F^+ centers[15–19] as electron traps; V'''_{Al}, V^-, and $V^=$ centers[20–23] as hole traps).

To test this proposition, a V^{4+},Mg^{2+}:Al_2O_3 sample was investigated. It was found that only one thermoluminescence peak (*d-d* red emission) was present at 210 K (trap depth: 0.60 eV). The TL excitation spectrum of the 210-K peak has a threshold that is the same as the one-step photoconductivity threshold at 300 nm. That is, the TL is due to trapped electrons. The different trap depth and peaking temperature between V^{4+}-doped and Ti^{3+}-doped sapphire suggest that the electron traps are not intrinsic defects of Al_2O_3, but probably characteristically associated with the dopant.

As mentioned in part I, 1 and 10% of the Ti exists as Ti^{4+} in sample *B* and sample *A*, respectively. Hence, the average Ti^{3+}-Ti^{4+} separation will be about 24 and 7.3 nm, respectively. These are both smaller than the "effective range" of electron in Onsager's model[24] (with an $\varepsilon_s = 10$ for Al_2O_3, the Onsager's radii are 28 nm at 300 K and 104 nm at 80 K). As a result, the electron will encounter Ti^{4+} before it is thermalized. The nonlocally compensated-uncompensated Ti^{4+} will recombine with the electron, forming Ti^{3+}. On the other hand, the compensated Ti^{4+} should be a shallow electron trap. Since the V'''_{Al} charge compensators (or substitutional Mg^{2+} for the doubly doped sample) have an effective negative charge in the lattice, they can modify the trapping cross section to a considerable extent, leading to a change in the trap depth and a shift in the thermoluminescence peak. Here we propose that the electron traps are probably the charge compensated Ti^{4+}.

As expected, no thermally stimulated conductivity was found for the Mg,Ti:Al_2O_3 since we can only detect signal from electron detrapping but the concentration of Ti^{3+} is low and also the average range of electrons is small because of the high Ti^{4+} concentration in sample *C*. Nevertheless, thermoluminescence of trapped holes is observable. Two broad peaks were found. To resolve these overlapping peaks, the temperature was fixed at the rising edge of the first peak until the signal subsided, then the temperature was raised again to record the second peak. After this, the first peak, was obtained by subtracting the second peak from the overlapping signal. The peaks appeared at 220 and 280 K. The estimated trap depths are 0.63 and 0.78 eV. Because of the negative effective charge of the Ti^{4+} charge compensators, it is assumed that they are the traps for the holes. This is justified as follows. The peaks in the doubly doped sample are much broader than the hole detrapping peak in the singly doped sample. Also, the trap depths are larger. The sharpness of the 168-K peak suggests that the trap distribution is very homogeneous, which is the case if the V'''_{Al} compensator is the nearest neighbor of the Ti^{4+} in the singly doped sample. Moreover, the trap is shallower because of the proximity of the titanium to the trapped hole (the shortest Al^{3+}-O^{2-} distance is 1.86 Å). On the other hand, the substitutional Mg'_{Al} in the doubly doped sample

has a lower negative charge compared to the V'''_{Al} compensator in the singly doped sample. As a result, the Coulombic attraction between the compensator and the Ti^{4+} is weaker. This leads to a broader distribution of the position of Mg^{2+} ions and hence the two broader, deeper traps.

IV. CONCLUSIONS

Locally and nonlocally charge compensated Ti^{4+} are identified. The large oscillator strength but long lifetime of the CT transition is explained by a spin-allowed absorption into a higher singlet state which is in thermal equilibrium with the lower triplet excited state.

The results from the thermally stimulated conductivity and thermoluminescence show the presence of electron traps and hole traps. Using two Mg^{2+}-codoped samples, the electron and hole traps are found to be associated with the dopant rather than the intrinsic defects of the host. It is suggested that the charge-compensated Ti^{4+} are the electron traps while the charge compensators for Ti^{4+} are the hole traps.

ACKNOWLEDGMENTS

We want to thank the Union Carbide Corporation and Steven Payne of the Lawrence Livermore National Laboratory for providing us with the crystals and Douglas Johnson of the Geology Department in Princeton University for preparing the crystal samples. The work was supported in part by the National Science Foundation under Grant No. EAR 89-17292 and by the Department of Chemistry. S.B.'s participation was made possible by a grant from the program Cooperation in Applied Science and Technology (CAST), administered by the National Research Council.

[1]W. C. Wong *et al.*, preceding paper, Phys. Rev. B **51**, 5682 (1995).
[2]W. C. Wong, D. S. McClure, and S. A. Basun, J. Lumin. **60&61**, 183 (1994).
[3]A. Sanchez, A. J. Strauss, R. L. Aggarwal, and R. E. Fahey, IEEE J. Quantum Electron. **24**, 995 (1988); R. L. Aggarwal, A. Sanchez, A. J. Strauss, W. R. Rapoport, and C. P. Khattak, *ibid.* **24**, 1003 (1988).
[4]B. Macalik, L. E. Bausa, J. Garcia-Sole, F. Jaque, J. E. Munoz Santiuste, and I. Vergara, Appl. Phys. A **55**, 144 (1992).
[5]L. E. Bausa, I. Vergara, F. Jaque, and J. Garcia Sole, J. Phys. Condens. Matter **2**, 9919 (1990).
[6]M. Yamaga, T. Yosida, S. Hara, N. Kodama, and B. Henderson, J. Appl. Phys. **75**, 1111 (1994).
[7]K. P. D. Lagerof, T. E. Mitchell, and A. H. Heurer, J. Am. Ceram. Soc. **72**, 2159 (1989).
[8]B. D. Evans, J. Lumin. **60&61**, 620 (1994).
[9]D. S. McClure, W. C. Wong, and S. A. Basun (unpublished).
[10]G. A. Dussel and R. H. Bube, Phys. Rev. **155**, 764 (1967).
[11]P. Dorenbos, S. Vrind, J. Dolfing, and H. W. den Hartog, Phys. Rev. B **35**, 5766 (1987).
[12]R. Capelletti, in *Defects in Solids: NATO Advanced Study Institute, Modern Techniques,* edited by A. V. Cadwick and M. Terenzi (Plenum, New York, 1986), p. 407.
[13]R. H. French, J. Am. Ceram. Soc. **73**, 477 (1990).
[14]B. J. Jeffries, J. D. Brewer, and G. P. Summers, Phys. Rev. B **24**, 6074 (1981).
[15]S. Y. La, R. H. Bartram, and R. T. Cox, J. Phys. Chem. Solids **34**, 1079 (1973).
[16]K. H. Lee and J. H. Crawford, Jr., Phys. Rev. B **15**, 4065 (1977).
[17]B. D. Evans and M. Stapelbroek, Phys. Rev. B **18**, 7089 (1978).
[18]B. G. Draeger and G. P. Summers, Phys. Rev. B **19**, 1172 (1979).
[19]J. H. Crawford, Jr., Semicond. Insulators **5**, 599 (1983).
[20]T. J. Turner and J. H. Crawford, Jr., Solid State Commun. **17**, 167 (1975).
[21]R. T. Cox, Solid State Commun. **9**, 1989 (1971).
[22]K. H. Lee, G. E. Holmberg, and J. H. Crawford, Jr., Solid State Commun. **20**, 183 (1976).
[23]K. H. Lee, G. E. Holmberg, and J. H. Crawford, Jr., Phys. Status Solidi A **39**, 669 (1977).
[24]L. Onsager, Phys. Rev. **54**, 554 (1938).